Universal nature and finite-range corrections in elastic atom-dimer scattering below the dimer breakup threshold

A. Kievsky[1] and M. Gattobigio[2]

[1]*Istituto Nazionale di Fisica Nucleare, Largo Pontecorvo 3, 56100 Pisa, Italy*

[2]*Université de Nice-Sophia Antipolis, Institut Non-Linéaire de Nice, CNRS, 1361 route des Lucioles, 06560 Valbonne, France*

(Received 14 December 2012; revised manuscript received 26 March 2013; published 31 May 2013)

We investigate universal behavior in elastic atom-dimer scattering below the dimer breakup threshold calculating the atom-dimer effective-range function $ak\cot\delta$. Using the He-He system as a reference, we solve the Schrödinger equation for a family of potentials having different values of the two-body scattering length a and we compare our results to the universal zero-range form deduced by Efimov, $ak\cot\delta = c_1(ka) + c_2(ka)\cot[s_0\ln(\kappa_* a) + \phi(ka)]$, for selected values of the three-body parameter κ_*. Using the parametrization of the universal functions c_1,c_2,ϕ given in the literature, a good agreement with the universal formula is obtained after introducing a particular type of finite-range corrections. Furthermore, we show that the same parametrization describes a very different system: nucleon-deuteron scattering below the deuteron breakup threshold. Our analysis confirms the universal character of the process, and relates the pole energy in the effective-range function of nucleon-deuteron scattering to the three-body parameter κ_*.

DOI: 10.1103/PhysRevA.87.052719 PACS number(s): 34.50.Cx, 31.15.xj, 25.45.De

I. INTRODUCTION

Scattering of two particles at very low energy shows universal behavior encoded in the scattering length a and in the effective range r_s. In fact, systems with different interactions sharing the same scattering length and the same effective range have the same effective-range function $k\cot\delta = -1/a + r_s k^2/2$, and, accordingly, the same low-energy behavior. In the limit $a \gg r_0$, where the scattering length is much greater than the typical range of the potential r_0, not only the scattering process is universal, but also some bound-state properties. When $a \to +\infty$ (known as unitary limit), the two-particle system has a shallow-bound state with the bound-state energy $E_2 \approx \hbar^2/ma^2$ fixed by the scattering length. In this limit, the physics is scale invariant.

In the 1970s, Efimov [1,2] showed that the scale invariance is broken in the s-wave three-body sector of a bosonic system. The residual symmetry is the discrete scale invariance (DSI), namely, the physics is invariant under the rescaling $r \to \Lambda^n r$, where the constant is usually written $\Lambda = e^{\pi/s_0}$, with $s_0 \approx 1.006\,24$ a universal number that characterizes a system of three identical bosons. One consequence is that at the unitary limit, the three-body spectrum consists of an infinite number of states that accumulate to zero with the ratio between two consecutive states being $E_3^{n+1}/E_3^n = e^{-2\pi/s_0}$. For finite scattering length, the binding energies satisfy the Efimov's equation

$$E_3^n + \frac{\hbar^2}{ma^2} = e^{-2(n-n_*)\pi/s_0}\exp\left[\Delta(\xi)/s_0\right]\frac{\hbar^2\kappa_*^2}{m}, \qquad (1)$$

with $\tan\xi = -(mE_3^n/\hbar^2)^{1/2}a$. The function $\Delta(\xi)$ is universal and a parametrization in the interval $[-\pi, -\pi/4]$ is given in Ref. [3]. The three-body parameter κ_* is the wave number of the $n = n_*$ state at the unitary limit.

The DSI constrains the form of the observables to be log-periodic functions of the control parameters. One example is the atom-dimer scattering length which has the general form

$$a_{AD}/a = d_1 + d_2\tan[s_0\ln(\kappa_* a) + d_3], \qquad (2)$$

where d_1,d_2,d_3 are universal constants whose value has been determined in the zero-range limit [3]. For collisions below the dimer breakup threshold, DSI imposes the following universal form for the effective-range function:

$$ka\cot\delta = c_1(ka) + c_2(ka)\cot[s_0\ln(\kappa_* a) + \phi(ka)], \qquad (3)$$

with δ the atom-dimer phase shift and c_1,c_2,ϕ universal functions of the dimensionless variable ka, where $k^2 = (4/3)E/(\hbar^2/m)$, being E the center-of-mass energy of the process. As $k \to 0$, $ka\cot\delta \to -a/a_{AD}$ and at $k = 0$ the constants d_1,d_2,d_3 and $c_1(0)$,$c_2(0)$,$\phi(0)$ are related by simple trigonometric relations. A parametrization of the universal constants and functions can be found in Ref. [3].

In this paper, we study in detail the universal behavior of a_{AD} and of the effective-range function $ka\cot\delta$. To this aim, we use the family of atomic ^{4}He-^{4}He potentials derived in Ref. [4] for several values of a, running from $a \approx 440\ a_0$ to $50\ a_0$. The corresponding dimer energies range from $E_2 \approx 0.22$ to 21 mK covering two orders of magnitude. For selected values of a in the mentioned interval, we calculate a_{AD} and the s-wave phase shift in order to construct the effective-range function below the dimer breakup threshold. As predicted by Eq. (3), when the value of a increases, we observe that a_{AD} changes sign tending to $-\infty$. This behavior produces a pole in the effective-range function. More specifically, our numerical results are used to analyze the universal form of Eqs. (2) and (3), and, as the calculations are done using finite-range interactions, to extract finite-range corrections by comparing our results to the zero-range theory. Interestingly, for the explored zone of positive scattering length, the range corrections can be taken into account by a shift in the variable $\kappa_* a$.

This study is of interest for several fields of research, ranging from cold atoms to nuclear physics and, in particular, in halo nuclei where a cluster description is justified. In atomic physics, where the Efimov effect has been observed for the first time [5], discrepancies arise between the theoretical prediction and the experimental determination of the ratio between a_*

and a_- [6,7], which means between the scattering lengths at which an Efimov state disappears in the atom-dimer and in the three-atom continua, respectively. The solution to this puzzle is probably hidden in finite-range corrections to the universal formulas (see Ref. [8] and references therein for a recent account of the problem). In halo nuclei there has been a lot of interest in the observation of universal aspects in the scattering of a neutron on a neutron-halo nucleus having a large scattering length, as for example the $n-{}^{19}$C system (see Refs. [9,10] and [11] for a recent review). In this context, we make use of the universal character of the effective-range function to evaluate a very different system: low-energy nucleon-deuteron scattering. It is well known that the nucleon-deuteron effective-range function presents a pole structure that has been related to the presence of a virtual state. First observations of this particular behavior have been done in Refs. [12–14], whereas in Ref. [15] an explicit calculation of the effective-range function has been done using a semirealistic nucleon-nucleon potential. In this last reference, the calculations allowed us to extract the energy of the pole after fitting the effective-range formula with the form suggested by Delves [16]. In this work, we show that the pole structure of the effective-range function can be quantitatively related to the universal form given by Eq. (3) and, using the parametrization determined in the atomic three-helium system, we apply that equation to describe nucleon-deuteron scattering as well. In particular, using the universal function ϕ, the energy of the pole can be used to extract the three-body parameter κ_*. In this way, the universal behavior imposed by the DSI is analyzed in systems with natural lengths that differ of several orders of magnitude.

II. THREE-BOSON MODEL

We construct the model using the LM2M2 [17], one of the most used ^{4}He-^{4}He potentials, as the reference interaction, with the mass parameter $\hbar^2/m = 43.281\,307(a_0)^2$ K. In order to change the value of the scattering length, we have modified the LM2M2 interaction as follows:

$$V_\lambda(r) = \lambda V_{\mathrm{LM2M2}}(r). \tag{4}$$

Examples of this strategy exist in the literature [18,19]. The unitary limit is produced for $\lambda \approx 0.9743$, whereas for $\lambda = 1$ the values of the LM2M2 are recovered: $a = 189.41\ a_0$, $E_2 = -1.303$ mK, and the effective range $r_s = 13.845\ a_0$.

Following Ref. [4], we define an attractive two-body Gaussian (TBG) potential

$$V(r) = V_0 e^{-r^2/r_0^2}, \tag{5}$$

with range $r_0 = 10\ a_0$ and strength V_0 fixed to reproduce the values of a given by $V_\lambda(r) = \lambda V_{\mathrm{LM2M2}}(r)$. For example, the strength $V_0 = -1.234\,356\,6$ K corresponds to $\lambda = 1$ reproducing the LM2M2 low-energy data $E_2 = -1.303$ mK, $a = 189.42\ a_0$, and $r_s = 13.80\ a_0$.

The use of the TBG potential in the three-atom system produces a ground-state binding energy appreciably deeper than the one calculated with $V_\lambda(r)$. For example, at $\lambda = 1$, the LM2M2 helium-trimer ground-state binding energy is $E_3^0 = 126.4$ mK, whereas the one obtained using the two-body soft-core potential in Eq. (5) is 151.32 mK. Hence, we introduce a repulsive hypercentral three-body (H3B) interaction

$$W(\rho_{123}) = W_0 e^{-\rho_{123}^2/\rho_0^2}, \tag{6}$$

with the strength W_0 tuned to reproduce the trimer energy E_3^0 obtained with $V_\lambda(r)$ for all the explored values of λ. Here, $\rho_{123}^2 = \frac{2}{3}(r_{12}^2 + r_{23}^2 + r_{31}^2)$ is the hyperradius of three particles and ρ_0 gives the range of the three-body force. Following Ref. [4], we use $\rho_0 = r_0$. It should be noticed that the description of the three-boson systems using a two- plus three-body interaction constructed to reproduce the low-energy data is equivalent, up to finite-range corrections, to a description based on effective field theory (EFT) at leading order (LO) [20].

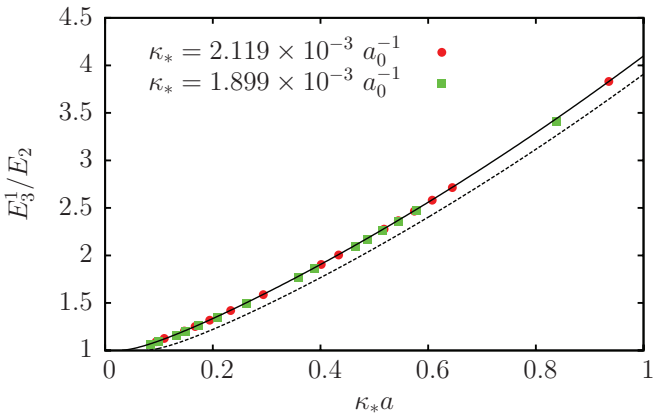

FIG. 1. (Color online) Energy of the first excited state of the trimer as a function of $\kappa_* a$. The dashed line is the universal prediction of the Efimov law, while the solid line is the translated universal curve. The full circles and full squares are the calculations using the TBG and TBG + H3B potentials, respectively.

Varying λ from the unitary limit to $\lambda = 1.1$, we obtain a set of values for the ground-state binding energy E_3^0 and first excited state E_3^1 using the TBG and TBG + H3B potentials in a broad interval of a. We use the results for E_3^1 at the unitary limit [by means of Eq. (1) with $n_* = 1$] to determine $\kappa_* = 0.002\,119\ a_0^{-1}$ and $\kappa_* = 0.001\,899\ a_0^{-1}$ for the TBG and TBG + H3B, respectively. In Fig. 1, we collect our results for the ratio E_3^1/E_2 as a function of $\kappa_* a$ for the TBG potential (full circles) and of the TBG + H3B potential (full squares). We compare the numerical calculations to the predictions of Efimov's binding energy [Eq. (1)] given in the figure by the dashed line. We observe that the numerical results lie on a curve shifted with respect to the dashed line. We can interpret the shift as a consequence of the finite-range character of the numerical results. Accordingly, we can adapt Efimov's equation to treat finite-range interactions. Once we fix $n_* = 1$, Eq. (1) can be rewritten as

$$E_3^1/E_2 = \tan^2\xi, \quad \kappa_*' a = \exp\left[-\Delta(\xi)/2s_0\right]/\cos\xi, \tag{7}$$

where we have introduced finite-range correction by $\hbar^2/ma^2 \to E_2$, in the two-body sector, and by a shift $\kappa_*' a = \kappa_* a + \Gamma$. Our calculations have been made for two different values of κ_*, allowing us to infer that in first approximation $\Gamma \approx \kappa_* r_*$, with $r_* = 21\ a_0 \approx 2r_0$. At the unitary limit, the relative weight of this shift becomes negligible, and Eq. (7) tends to Eq. (1).

TABLE I. The atom-dimer scattering length a_{AD} (in units of a_0) in terms of the number of Laguerre polynomial m and the grand angular quantum number K.

m/K	120	240	360	480
24	169.64	165.40	165.23	165.22
28	169.59	165.32	165.10	165.09
32	169.55	165.28	165.05	165.04
36	169.54	165.27	165.04	165.02
40	169.53	165.26	165.03	165.02

Equation (7) can be generalized to states different from the first excited; however, the shift in this case will also depend on the size of the state and will not be negligible at the unitary limit. The corresponding results, obtained by solving Eq. (7) with $\kappa_*' a = \kappa_* a + \kappa_* r_*$, are shown in Fig. 1 as a solid line.

III. ATOM-DIMER SCATTERING

To describe atom-dimer scattering below the dimer threshold we calculate a_{AD} and the s-wave atom-dimer phases δ using the TBG and TBG + H3B potentials at different energies. We use the hyperspherical harmonic (HH) method in conjunction with the Kohn variational principle [21]. Applications of the method to describe a three-helium system with soft-core interactions as used here can be found in Ref. [22]. As an example, in Table I the a_{AD} convergence pattern is given for $\lambda = 1$ using the TBG potential. The results for a_{AD} are studied in terms of the size of the HH basis given by the grand orbital quantum number K and the quantum number m of the hyperradial basis (here taken as Laguerre functions [21]). When the TBG + H3B potential is considered, the rate of convergence remains the same and the final value is 208 a_0. It should be noticed that as a increases, and correspondingly $|E_2|$ diminishes, is necessary to increase the size of the basis. At the largest value of a considered, $a \approx 441\ a_0$, we have used a basis with $m = 60$ and $K = 800$.

Defining $E_2 = \hbar^2/m a_B^2$, in Fig. 2 we show the results for the ratio a_{AD}/a_B in terms of the product $\kappa_* a$. It can be observed that the calculated points, given as full circles (TBG potential) and full squares (TBG + H3B potential), lie on a curve shifted with respect to the dashed line representing Eq. (2) with the parametrization of Ref. [3]. We can interpret again the shift as produced by the finite-range character of the calculations. Accordingly, we can adapt Eq. (2) to describe finite-range interaction as

$$a_{AD}/a_B = d_1 + d_2 \tan[s_0 \ln(\kappa_*' a) + d_3]. \tag{8}$$

In fact, replacing in the above equation $\kappa_*' a = \kappa_* a + \kappa_* r_*$ with the same numerical value of r_* as before, the solid line is obtained in Fig. 2. The values $d_1 = 1.531$, $d_2 = -2.141$, $d_3 = 1.100$ slightly modify the parametrization of Ref. [3] to better describe the numerical results. This new parametrization is shown as a dotted line in the figure where we can observe an improvement in the description of the results close to the unitary limit.

The shifted formula can be used to determine the ratio a_*/a_-, where a_- is the scattering length at which the three-body states disappear into the three-atom continuum, and a_* is the scattering length at which the three-body states disappear into the atom-dimer continuum. For the potential models used in this work, the values of a_- are given in Ref. [4] whereas the values of a_* can be extracted by equating the argument of the tangent in Eq. (8) to $-\pi/2$. Using these inputs, we obtain $a_*/a_- \approx -0.32$ for both $\kappa_* = 0.002\,119\ a_0^{-1}$ and $\kappa_* = 0.001\,899\ a_0^{-1}$. The zero-range universal formulas (1) and (2) predict $a_*/a_- = -1.07$, but recent experimental results give lower values for this ratio [6,7]. The difference is given by finite-range effects [23–27], which in our case are encoded in the shift.

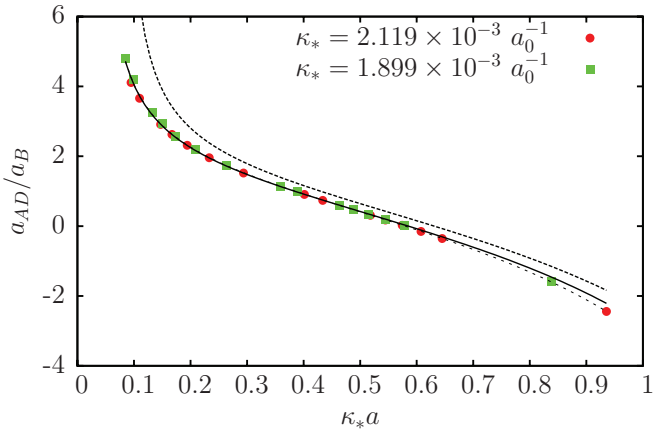

FIG. 2. (Color online) Universal plot for a_{AD}/a_B in terms of $\kappa_* a$. Open circles and open squares correspond to TBG and TBG + H3B potentials, respectively. The dashed line corresponds to Eq. (2), whereas the solid line corresponds to Eq. (8). The dotted line shows the present parametrization of Eq. (8).

It is interesting to see that the finite-range corrections cancel in the description of the scattering length as a function of the trimer energy. This is shown in Fig. 3 in which the present calculations and the zero-range universal theory, Eqs. (1) and (2), are in close agreement.

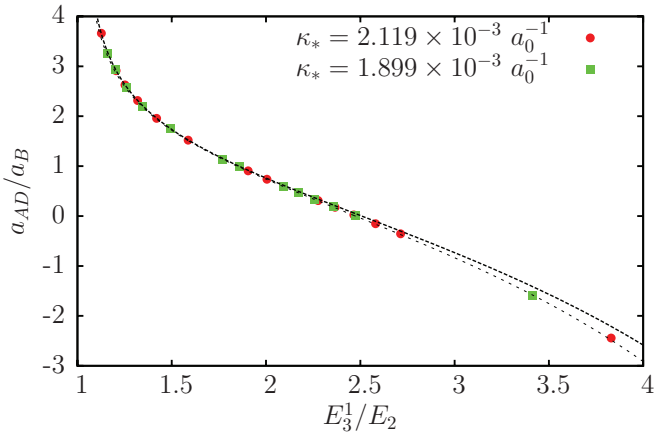

FIG. 3. (Color online) The ratio a_{AD}/a_B as a function of E_3^1/E_2. Open circles and open squares correspond to TBG and TBG + H3B potentials, respectively. The dashed line corresponds to Eq. (2) with the parametrization of Ref. [3], whereas the dotted line shows the present parametrization of Eq. (8).

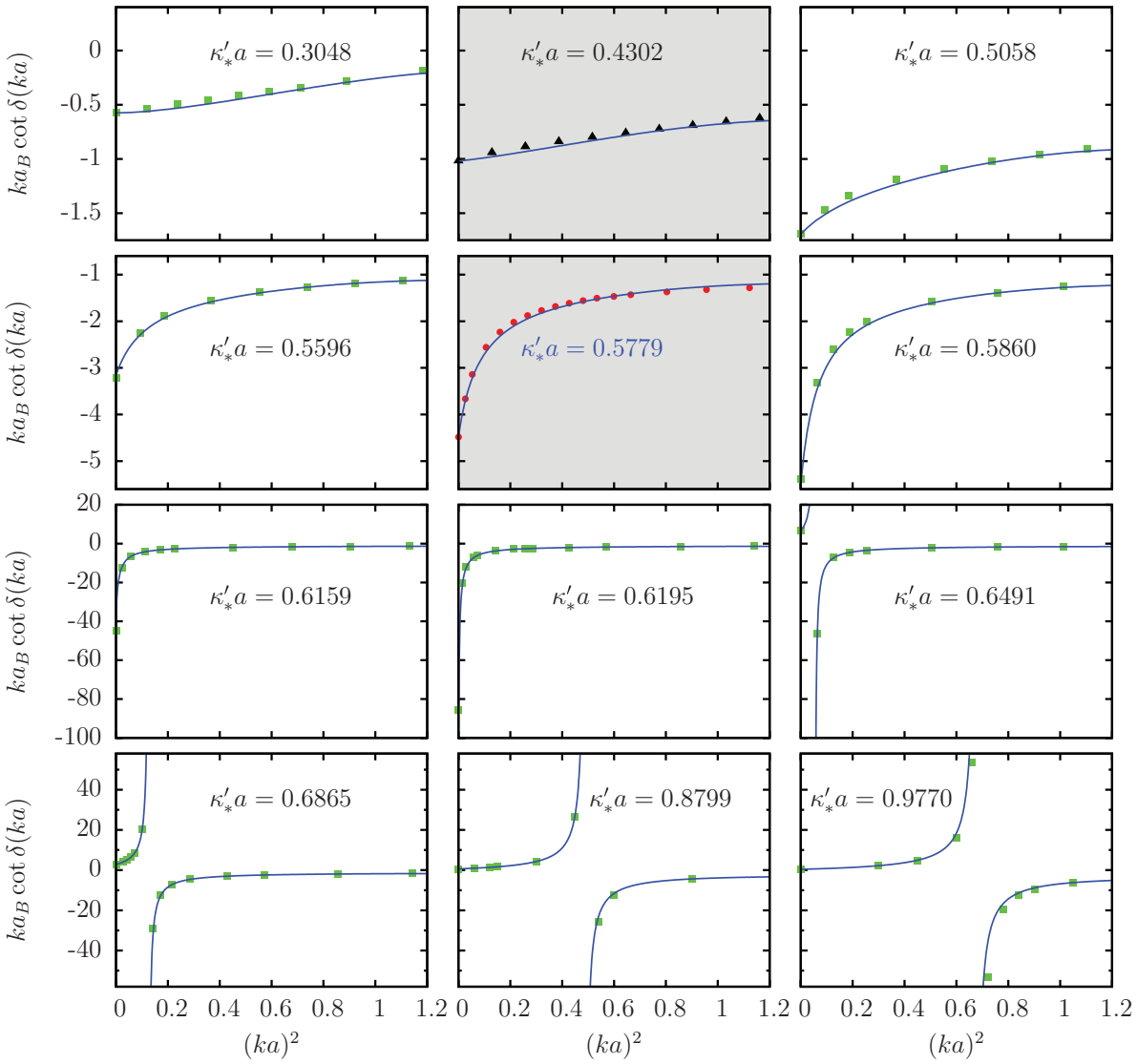

FIG. 4. (Color online) The effective-range function at different values of $\kappa_* a$ as a function of $(ka)^2$. The square points are our calculations; the triangle points are the calculations for real ^{4}He-^{4}He$_2$ scattering. The full circles, for $\kappa_* a = 0.543\,055$, correspond to neutron-deuteron scattering in the doublet channel. The solid curves have been calculated using the translated universal formula for the different values of $\kappa_* a$.

We now present results for atom-dimer scattering at energies below the dimer breakup threshold for different values of a. We adapt Eq. (3) to finite-range interactions by considering $ka_B \cot\delta$ as a function of the dimensionless center-of-mass energy $(ka)^2$ and using $\kappa'_* a = \kappa_* a + \kappa_* r_*$ in the argument of the logarithm function:

$$ka_B \cot\delta = c_1(ka) + c_2(ka)\cot[s_0 \ln(\kappa'_* a) + \phi(ka)]\,. \quad (9)$$

In Fig. 4 we show our results (given as full squares) at different values of $\kappa'_* a$. In the figure, we can observe very different patterns. For the smallest values of $\kappa'_* a$, the behavior is almost linear in all the energy ranges. Starting at values of $\kappa'_* a \approx 0.4$, a curvature appears close to zero energy, pointing out to an emergent pole structure that becomes evident at larger values of $\kappa'_* a$. Specifically, the pole appears when a_{AD} changes sign (see Fig. 2) or, as given in Eq. (9), when the argument of the cotangent function becomes zero (or $n\pi$). The shadow plot in the first row of Fig. 4 corresponds to the case $\lambda = 1$ and describes ^{4}He-^{4}He$_2$ scattering (full triangles). The shadow plot in the second row corresponds to nucleon-deuteron scattering as discussed below. The solid curves are obtained using the finite-range-adapted equation (9) with the parametrization of Ref. [3]. We can observe a noticeable agreement along the whole range of values.

IV. NUCLEON-DEUTERON SCATTERING

The universal effective-range function has been determined using the TBG and the TBG + H3B potentials describing an atomic three-helium system. The universal character of the function allows us to apply it to describe a very different system: nucleon-deuteron (n-d) scattering. Many efforts have been given in the past to understand the peculiar form of the n-d effective-range function at low energies (see Refs. [12–14]). However, Efimov showed that this process can be described with the universal formula of Eq. (3) [28]. Accordingly, we

would like to apply Eq. (9) to perform a quantitative description of n-d scattering at low energies. To this aim, we use the results of Ref. [15] in which n-d scattering has been described using a spin-dependent central potential. In that reference, they obtained $a_{nd} = 0.71$ fm for the n-d scattering length, and the effective-range function has been parametrized as

$$k \cot \delta = \frac{-1/a_{nd} + r_s k^2/2}{1 + E_{\mathrm{c.m.}}/E_p} \tag{10}$$

with $E_p = -160$ keV and $r_s \approx -127$ fm. It should be noticed that this particular parametrization of the effective-range function can be simply related to Eq. (9) in the low-energy limit. Accordingly, from the values of E_p and a_{nd} it is possible to determine the corresponding values of a and κ_*' by using the universal function ϕ and Eq. (8). We obtain $a = 4.075$ fm and $\kappa_*' a = 0.5779$. The pole appears in the negative region similar to what happens in Fig. 4 at intermediate $\kappa_*' a$ values. The shadow panel of the second row in Fig. 4 shows a comparison of the universal function (solid line) to the n-d scattering results of Ref. [15] (full circles). We observe a noticeable agreement. It should be noticed that the spin-dependent potential used in Ref. [15] reproduces the singlet (${}^1a_{np} \approx -20$ fm) and triplet (${}^3a_{np} \approx 5$ fm) n-p scattering lengths. Accordingly, the three-nucleon systems have a symmetric plus a mixed symmetry component. The value of a extracted from the universal function, which is close to ${}^3a_{np}$, can be considered an effective value in an equivalent three-boson system with the given a_{nd} and the corresponding effective-range function. A deeper analysis extending the model to spin-dependent interactions is at present underway.

This study could be of interest in light neutron halo systems in which a low-energy neutron can impact on a loosely bound n-core system. For example, specific applications of Eq. (3) recently appear in low energy $n - {}^{19}$C scattering [10]. We expect that the use of Eq. (3) will be useful in further studies of such systems.

V. CONCLUSIONS

In this work, we have analyzed the low-energy behavior of a three-boson system in which the interaction between two bosons produces a large scattering length. Following Ref. [4], we have used the three-helium system as a reference system and, in the spirit of EFT at LO, we have constructed an attractive two-body interaction plus a repulsive three-body interaction devised to reproduce the two-body scattering length and three-body binding energy of the LM2M2 interaction. From our numerical results we have shown that, when finite-range interactions are used, the zero-range universal formula has to be adapted, introducing a shifted three-body parameter $\kappa_*' a = \kappa_* a + \kappa_* r_*$. This is a particular type of range correction and the numerical value of $r_* \approx 2r_0$, in the case of the helium system, has been extracted from our calculations. We have proposed and solved Eq. (7) to describe the spectrum of a three-boson system. This equation can be considered an extension of Eq. (1) for finite-range interactions; they are characterized by two parameters, the effective range r_s (in the relation between E_2 and a) and the shift r_*, that are somehow connected. Their relation is at present subject of investigation.

In the case of atom-dimer scattering, we have proposed Eqs. (8) and (9) introducing the shifted parameter κ_*'. In order to describe our numerical results, we have used the parametrization of Ref. [3], which, without the inclusion of the shift, can not quantitatively describe the very complicated structure of the effective-range function. Interestingly, the value of r_* necessary to describe the results is the same for E_3^1, for a_{AD}, and for the effective-range function. This type of correction can be compared to the range corrections obtained in very recent works [29,30].

As a second application, we have used Eq. (9) to describe low-energy n-d scattering. The values of κ_*' and a entering in the equation have been determined from the pole energy E_p and the doublet scattering length a_{nd} given in Ref. [15]. A quantitative agreement between a direct application of Eq. (9) and the calculations on the n-d system has been found. This analysis connects the universal behavior of atomic systems having large two-body scattering length to nuclear systems. Work in progress includes the extension of the present analysis to energies above the dimer breakup, in particular, the description of the recombination rate at threshold, and the extension to include spin and isospin degrees of freedom in order to consider nuclear systems.

[1] V. Efimov, Phys. Lett. B **33**, 563 (1970).
[2] V. Efimov, Sov. J. Nucl. Phys. **12**, 589 (1971) [Yad. Fiz. **12**, 1080 (1970)].
[3] E. Braaten and H. Hammer, Phys. Rep. **428**, 259 (2006).
[4] M. Gattobigio, A. Kievsky, and M. Viviani, Phys. Rev. A **86**, 042513 (2012).
[5] T. Kraemer, M. Mark, P. Waldburger, J. G. Danzl, C. Chin, B. Engeser, A. D. Lange, K. Pilch, A. Jaakkola, H. Nägerl, and R. Grimm, Nature (London) **440**, 315 (2006).
[6] M. Zaccanti, B. Deissler, C. D'Errico, M. Fattori, M. Jona-Lasinio, S. Müller, G. Roati, M. Inguscio, and G. Modugno, Nat. Phys. **5**, 586 (2009).
[7] O. Machtey, Z. Shotan, N. Gross, and L. Khaykovich, Phys. Rev. Lett. **108**, 210406 (2012).
[8] P. Dyke, S. E. Pollack, and R. G. Hulet, arXiv:1302.0281.
[9] I. Mazumdar, A. R. P. Rau, and V. S. Bhasin, Phys. Rev. Lett. **97**, 062503 (2006).
[10] M. Yamashita, T. Frederico, and L. Tomio, Phys. Lett. B **670**, 49 (2008).
[11] T. Frederico, A. Delfino, L. Tomio, and M. Yamashita, Prog. Part. Nucl. Phys. **67**, 939 (2012).
[12] G. Barton and A. Phillips, Nucl. Phys. A **132**, 97 (1969).
[13] J. S. Whiting and M. G. Fuda, Phys. Rev. C **14**, 18 (1976).
[14] B. A. Girard and M. G. Fuda, Phys. Rev. C **19**, 579 (1979).
[15] C. R. Chen, G. L. Payne, J. L. Friar, and B. F. Gibson, Phys. Rev. C **39**, 1261 (1989).
[16] L. M. Delves, Phys. Rev. **118**, 1318 (1960).
[17] R. A. Aziz and M. J. Slaman, J. Chem. Phys. **94**, 8047 (1991).

[18] B. D. Esry, C. D. Lin, and C. H. Greene, Phys. Rev. A **54**, 394 (1996).
[19] P. Barletta and A. Kievsky, Phys. Rev. A **64**, 042514 (2001).
[20] P. F. Bedaque, H.-W. Hammer, and U. van Kolck, Phys. Rev. Lett. **82**, 463 (1999).
[21] A. Kievsky, Nucl. Phys. A **624**, 125 (1997).
[22] A. Kievsky, E. Garrido, C. Romero-Redondo, and P. Barletta, Few-Body Syst. **51**, 259 (2011).
[23] T. Frederico, L. Tomio, A. Delfino, and A. E. A. Amorim, Phys. Rev. A **60**, R9 (1999).
[24] P. Naidon and M. Ueda, C. R. Phys. **12**, 13 (2011).
[25] C. Ji, D. R. Phillips, and L. Platter, Europhys. Lett. **92**, 13003 (2010).
[26] J. P. D'Incao, C. H. Greene, and B. D. Esry, J. Phys. B: At., Mol. Opt. Phys. **42**, 044016 (2009).
[27] M. Thøgersen, D. V. Fedorov, and A. S. Jensen, Phys. Rev. A **78**, 020501 (2008).
[28] V. Efimov, Sov. J. Nucl. Phys. **29**, 546 (1979) [Yad. Fiz. **29**, 1058 (1979)].
[29] L. Platter, C. Ji, and D. R. Phillips, Phys. Rev. A **79**, 022702 (2009).
[30] P. K. Sørensen, D. V. Fedorov, A. S. Jensen, and N. T. Zinner, Phys. Rev. A **86**, 052516 (2012).